ITU - Telecommunication Standardization Sector

Temporary Document 2016-04-Q4-021

Original: English

STUDY GROUP 15

Berlin, Germany – April 2016

Question: 4/15

SOURCE1: TNO

TITLE: G.vector: Understanding and modelling the dual slope effect on EL-FEXT

ABSTRACT

This contribution is a covering letter for an attached paper, submitted to IEEE for possible publication, that elaborates on the cause of the dual-slope behavior of far end crosstalk. The attached paper clarifies it via a full multi-port model of a twisted pair quad cable, and shows a good match between that model and cable measurements. Since a full multi-port approach may not be convenient for all studies, we also propose the use of a simplified model for VDSL and G.fast performance studies, which is essentially an extension to the legacy ETSI model for EL-FEXT.

1. Introduction:

Various items in the issue list for G.vector are related to crosstalk, including the implicit demand for improved crosstalk channel modelling (4.x) and mitigating strong FEXT levels (2.1.2, 2.1.3, 2.1.4, 2.2.1, etc). The same applies for the issue list for G.fast, which explicitly calls for papers on FEXT and noise models above 30 MHz.

One of the reasons why these FEXT levels are getting so strong is that above a certain frequency the EL-FEXT increases with 40 dB/decade instead of the usual 20 dB/decade. This effect was raised in our ITU contribution of February 2012 [2] and called the "dual slope effect". Since then the existence of that "dual slope" effect was reconfirmed by many others and observed in various different cables [3,4,5,6,7,8,9,10,12,13,14,15]. This all shows the need for putting strong demands on vectoring engines to handle these high noise levels as well [16]. So far the phenomenon was not well understood and resulted in a number of conjecture explanations [11] in Broadband Forum as well as in ITU-T. As a result it was not clear how to model that and how the far end crosstalk changes with the loop length. But it is obvious that the legacy ETSI model for FEXT [17] is not adequate anymore for frequencies where this dual slope effect occurs.

This contribution is to clarify the physical cause of the dual slope effect, by means of a full multi-port model. This model facilitates studies on how that effect changes when changing different design parameters of cables and to show that the slope of this second order effect is 40 dB/decade over a wide frequency interval. And since a full multi-port model is not always convenient for performance studies, we also propose the use of a simplified generic model, which describes EL-FEXT pretty well for arbitrary cable lengths and is controlled by only two (empirical) parameters.

1

Author: Rob van den Brink TNOTel: +31 88 86 67059

Email: rob.vandenbrink@tno.nlContact:Bas van den Heuvel

TNOTel: +31 88 86 67126 Email: bas.vandenheuvel@tno.nl

2. Full modelling of the dual slope behavior of EL-FEXT

A detailed analysis of the dual slope effect is described in [1], a paper which is recently submitted to IEEE for possible publication, and that is attached to this contribution. That paper demonstrates that the dual slope effect of EL-FEXT is a combination of a first order effect (20 dB/decade) caused by (well known) random imperfections in the symmetry of the wiring and a second order residual effect (40 dB/decade) that is deterministic in nature. And that second order effect dominates above a certain break frequency until the EL-FEXT approximates zero dB.

That second order effect is caused by the interaction between the twist in the wires and its metallic surroundings (e.g. shield). The twist reduces the crosstalk due to capacitive unbalance significantly by balancing the capacitive coupling to its metallic surroundings on *average*. But a residual EL-FEXT term remains due to the repetitive/alternating variations around an average capacitance to surroundings. And that residual term happens to increase with 40 dB/decade, and becomes visible as a the dual slope effect when it dominates the first order effect.

The paper in [1] uses a full multi-port approach to model the twist, and demonstrates that such an approach can offer a very good match between model and measurements, as shown in figure 1. Both transmission and FEXT are well predicted by the model, and even the dip in transmission near 64 MHz is predicted quite well.

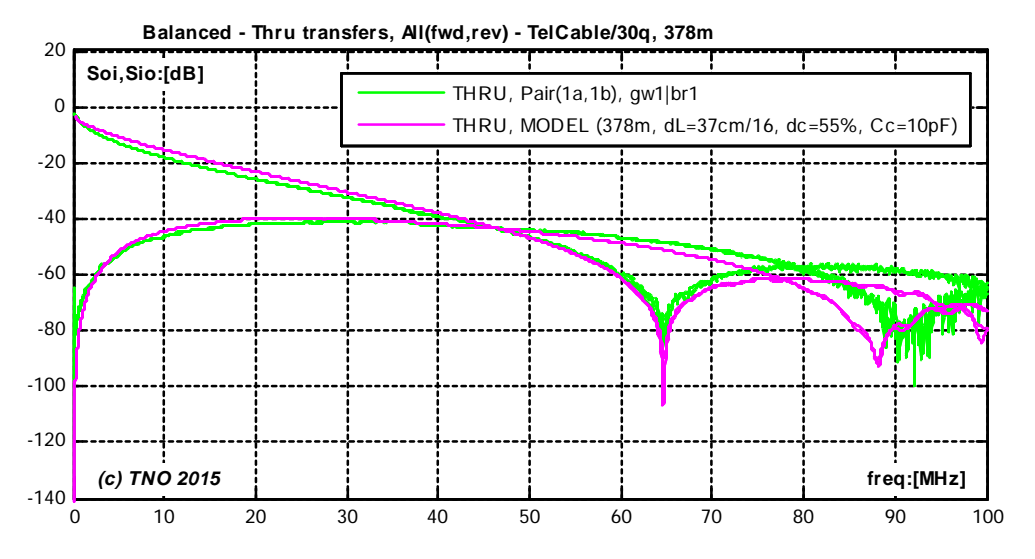


Figure 1 Match between a sample cable measurement and the full multi-port model proposed in [1]. Both transmission and FEXT are well predicted by the model, and this even applies to the dip in transmission near 64 MHz.

The full multi-port model is subsequently used in [1] to show how much the magnitude of the second order EL-FEXT changes with cable design parameters like twist length and capacitance to shield. But in all cases the slope of that second order effect is exactly 40 dB/decade up to a frequency where the EL-FEXT approaches zero dB.

3. Simplified modelling of the dual slope behavior of EL-FEXT

Our full multi-port model may be too complicated for studying modem performance in cables and therefore we propose an additional but simplified EL-FEXT model for such studies. It appears like an extension to the legacy ETSI model for EL-FEXT [17] and requires only one additional parameter value to specify the EL-FEXT for arbitrary cable lengths. The legacy ETSI model [17] for EL-FEXT has the following characteristics:

- The crosstalk effect has a slope of exactly 20 dB/decade.
- The presence of a second order effect is lacking.
- The crosstalk becomes unrealistic high for high frequencies since it keeps growing above 0dB.
- The magnitude of the crosstalk scales with the root of the cable length.

Our (simplified) model proposed in [1] fulfills at least the following requirements:

- The first order crosstalk effect has a slope of exactly 20 dB/decade.
- The second order crosstalk effect has a slope of exactly 40 dB/decade.
- The EL-FEXT does not exceeds levels above 0 dB.
- The magnitude of the first order crosstalk effect scales with the root of the cable length.
- The magnitude of the second order crosstalk effect scales proportional with the cable length.

Figure 2 and 3 show the desired behavior of our (simplified) model for two different cable lengths.

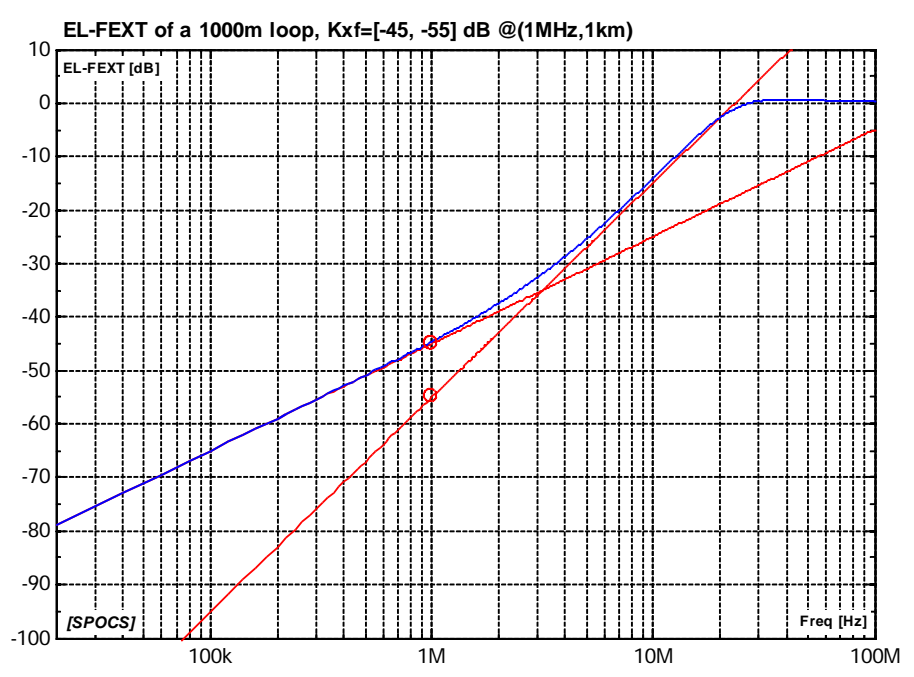


Figure 2. Crosstalk prediction of the proposed EL-FEXT model, for a 1km loop, when the model is characterized as K_{xfl} = -45 dB and K_{xf2} = -55 dB, both specified at 1 MHz and 1km. The asymptotes are crossing at 1 MHz the values of K_{xf1} and K_{xf2} since it is a 1 km loop.

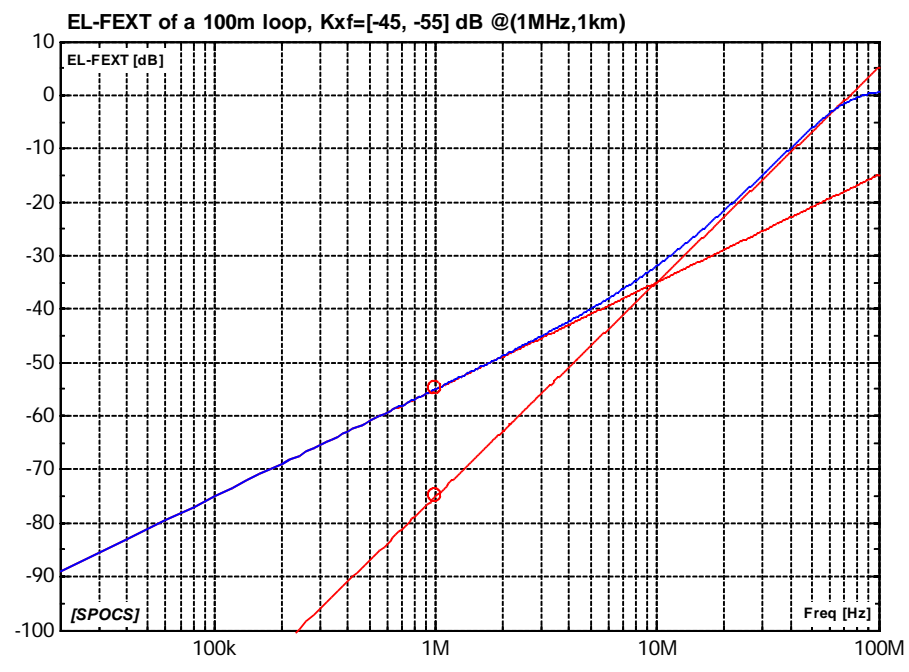


Figure 3. Crosstalk prediction of the proposed EL-FEXT model for a 100m loop, using the same parameter values as in figure 2. Since the vertical offset of both asymptotes scale differently with the cable length, the break frequency in this figure (10 MHz) is different from its value in the previous figure (3 MHz).

The model prevents that the maximum coupling increases 0 dB at high frequencies.

Our model used in figure 2 and 3 is expressed as the transfer function of a second order high-pass filter via:

$$H_{ELFEXT}(jw, L) = \frac{k_1(L) \cdot \left(\frac{jw}{w_0}\right) + k_2(L) \cdot \left(\frac{jw}{w_0}\right)^2}{1 + \left(k_1(L) + \sqrt{k_2(L)}\right) \cdot \left(\frac{jw}{w_0}\right) + k_2(L) \cdot \left(\frac{jw}{w_0}\right)^2}$$

Where
$$k_1(L) = K_{XF1} \cdot \sqrt{(L/L_0)}$$
, and $k_2(L) = K_{XF2} \cdot (L/L_0)$

If we normalize this formula with $L_0 = 1 \text{km}$ and $\omega_0 = 2\pi \cdot 1$ MHz and obtain values for K_{XF1} and K_{XF2} via measurements on a single cable length, then the model is fully specified for all cable lengths.

4. Summary

This paper should be presented under the G.vectoring agenda and/or the G.FAST agenda. It is related to the issues 2.1.x and 2.2.1 on the G.vector issue list, and to the call for papers papers on FEXT and noise models above 30 MHz on the G.fast issue list

The attached paper [1] to this contribution explains the cause of the dual slope effect in far end crosstalk and shows how that second order effect changes with various design parameters of cables and the cable length. This second order effect is deterministic in nature (opposite to the well-known random behaviour of the first order effect) and its magnitude scales therefore proportionally with the cable length (opposite to the well-known scaling with the root of the cable length of the first order effect).

In addition to the full multi-port model being used we also propose a more simplified model offering a fair prediction of the magnitude of the EL-FEXT for arbitrary loop lengths.

This contribution is for information.

5. References

- [1] Rob F.M. van den Brink, "Modelling the dual-slope behavior of EL-FEXT in twisted-pair quad cables" Submitted to IEEE for possible publication, January 2016.
- [2] TNO (Rob van den Brink, Bas van den Heuvel), "Dual slope behavior of EL-FEXT", contribution 2012-02-4A-038 to ITU-T-SG15/Q4, Feb 2012.
- [3] Brink, "Far-End crosstalk in twisted pair cabling: measurements and modeling", TNO Contribution 11RV-022, ITU-T SG15/Q4, Nov 2011.
- [4] Eriksson, Berg, Lu; "Equal Length FEXT measurements on PE05 cable", Ericsson Contribution 11RV-054R1, ITU-T SG15/Q4, Richmond, November 2011.
- [5] Huawei, "Equal-Length FEXT Measurements on PE05 Cable", Huawei Contribution COM 15 C 1864, ITU-T SG15/Q4, November 2011.
- [6] Bruyssel, Maes "Dual *slope behaviour of EL-FEXT*", ALU Contribution 2012-06-4A-033, ITU-T SG15/Q4, May 2012.
- [7] Humphrey, "On dual slope FEXT observations", BT Contribution 2012-05-4A-021, ITU-T SG15/Q4, May 2012.
- [8] Humphrey, Morsman, "FEXT cable measurements", BT Contribution 2012-05-4A-025, ITU-T SG15/Q4, May 2012.
- [9] Muggenthaler, Tudziers; "EL-FEXT Analysis", DT Contribution 2012-06-4A-041, ITU-T SG15/Q4, May 2012.
- [10] Bongard, "Dual slope ELFEXT behaviour on Swiss cables", Swisscom contribution 2013-01-Q4-042, ITU-T SG15/Q4, Feb 2013.
- [11] Schneider, Kerpez, Starr, Sorbara "*Transfer Functions, Input Impedance and Noise Models for the Loop End*", Cosigned contribution bbf2014.066.00, BroadbandForum, March 2014.
- [12] Kozarev, Strobel, Leimer, Muggenthaler, "*Modeling of Twisted-Pair Quad Cables for MIMO Applications*" Lantiq/DT Contribution bbf2014.467, BroadbandForum, june 2014 (updated from bbf2014.377 and bbf2014.117).
- [13] Heuvel, Trommelen, Brink, "G.fast: Preliminary analysis of the transfer characteristics of the 104 m KPN Access cable", TNO Contribution 2013-03-Q4-026, March 2013
- [14] Heuvel, "G.vector: High in-quad crosstalk coupling in older cables", TNO Contribution 2015-10-Q4-024, ITU-T SG15/Q4, Oct 2015.
- [15] Heuvel, "G.vector: High crosstalk coupling in older cables Measurements on GPLK01", TNO Contribution 2015-11-Q4-028, ITU-T SG15/Q4, Dec 2015.
- [16] Heuvel, "G.vector: Vectoring for VDSL2/35b must be able to deal with the high crosstalk coupling present in older cables", TNO Contribution 2015-10-Q4-023, Oct 2015
- [17] ETSI TR 101 830-2, Spectral Management on metallic access networks, Part 2: Technical methods for performance evaluations, revision V1.2.1, 2008.

Modeling the dual-slope behavior of EL-FEXT in twisted pair quad cables

Rob F.M. van den Brink

Abstract—It is well known that crosstalk in telephony cabling increases with the frequency, and transmission systems like VDSL and G.fast are designed to cope with that. But the awareness that the increase of EL-FEXT (equal level - far end cross talk) becomes much stronger above a certain frequency (increases with 40 instead of 20dB per decade) was raised only recently in ITU and BBF standardization bodies for G.fast. This phenomenon became known under the name "dual slope" effect, was initially not well understood, and resulted in a number of conjectured explanations. This paper demonstrates that the dual slope effect is deterministic in nature, and is caused by the interaction of the twist in the wires and its metallic surroundings (e.g. shield). Especially the repetitive variation of capacitance between (twisted) wire and shield adds that extra slope of 40 dB/decade to the far end crosstalk. This paper proposes a model and quantifies with that how sensitive this effect is to cable design parameters like twist length and capacitance to shield. In addition, an extension is proposed to a commonly used simplified system model for predicting the far end cross talk as a function of the frequency and cable length.

Index Terms—Twisted pair cables, far-end crosstalk, transmission line theory, cable modeling, digital subscriber line (DSL)

1 Introduction

SL modems (Digital Subscriber Line), aimed for the next generation broadband via copper [1], are designed to transmit their signals through multi-pair telephony cables under noisy stress conditions. This noise originates via crosstalk from other DSL systems using other wire pairs in the same cable. Most of this crosstalk can be eliminated by proper vectoring techniques, a technique that has become common within DSL systems, and required by G.fast and VDSL standards. But these crosstalk levels increase with the frequency and can even exceed the level of the DSL signals beyond some break-frequency at given cable length [2]. This puts strong demands on vector engines to handle these high noise levels as well. G.fast can transmit signals up to 106MHz (and in future up to 212 MHz) and recent version of VDSL up to 35 MHz, and these frequencies required the development of more advanced models for twisted pair cables up to hundreds of MHz [3], [4], [5]. Legacy models on crosstalk [6] assume that the

Rob F.M. van den Brink is with TNO, Den Haag, The Netherlands, e-mail: Rob.vandenBrink@tno.nl.

This work has been submitted to the IEEE for possible publication. Copyright may be transferred without notice, after which this version may no longer be accessible.

ratio between far end crosstalk and transmission (the equal level FEXT, or just EL-FEXT) increases in frequency with a slope of 20dB/decade and increases in length with the square-root of the cable length [6], [7]. But more recent measurements focused on higher frequencies uncovered a dualslope behavior of the EL-FEXT [2], [8], [9] showing a second order crosstalk effect of 40dB/decade as well. This effect doubles the slope of noise above some break frequency and becomes dominant thereafter. And since this effect also increases proportionally with the cable length (instead of with the square root of it) it is an effect that has significant impact on the usability of higher frequency bands by DSL systems and their vectoring engines. As soon as we raised [9], [8] the awareness of this effect in ITU-T SG15/Q4, the standardization body for VDSL and G.fast, the presence of a dual slope in other telephony cables was soon reconfirmed by several others [10], [11], [12], [13], [14], [15], [16] in ITU and Broadband Forum. Initially the cause was not wellunderstood, and this resulted in a number of conjectured explanations for the dual slope effect (well summarized in [17]:sect5.2). Although one of the ITU contribution [15] related the dual slope effect to the twist of the wires and the shield, a good understanding on how the characteristics of this second order effect relates to various cable characteristics remained lacking. (This was partly due to the language barrier, since [15] was phrased in German). In this paper, chapter 2 start with demonstrating the existence of this second order effect in EL-FEXT via measurements. Chapter 3 elaborates on a full eight-port model to study the impact of twisting four wires in the vicinity of a shield. Chapter 4 shows how reliable this modeling is and chapter 5 analyses how sensitive the second order slope is to various design parameters of a cable. Our eight-port model is quite reliable but too complicated for simple system calculations on modem performance. Therefore we propose in chapter 6 an extension to a commonly used simplified model for EL-FEXT to cover the second slope and associated lengthdependency as well.

2 MEASUREMENT RESULTS

To illustrate the dual slope effect, we selected a characterization [2] of a multi-pair telephony cable, 378m in length and winded on a drum, where the wires are organized in groups of four (30 twisted quads in total, similar to figure 4) and where the cable has a common shield. Measurements were

performed directly on the individual wires (using the shield as common) by means of an 8-port network analyzer, without balanced transformers and with full 8-port correction of systematic measurement errors [2], [18]. Balanced mode transmission and crosstalk curves were mathematically extracted from these single wire measurements, and the results are shown in figure 1 to 3. Figure 1 shows two curves, the upper curve "TRAN" representing the measured balanced transmission in a wire pair of a quad, and the lower curve "FEXT" representing the far end crosstalk to that wire pair from the other pair in the quad. The FEXT increases with the frequency, and beyond about 50MHz the crosstalk levels are even higher than the direct transmission levels. Figure 2 shows a curve "ELFEXT" representing the magnitude of the ratio between measured "FEXT and "TRAN from figure 1. This ratio is called the "equal level FEXT". Two additional asymptotic lines, labeled as "slope 1" (of 20 dB/decade) and "slope 2" (of 40 dB/decade), are drawn to highlight the dual slope effect of this EL-FEXT curve. The asymptotic lines cross each other near 2 MHz, but that break frequency is cable, quad and length dependent. So the second slope becomes dominant above about 2 MHz in this example, and affects almost the full VDSL band.

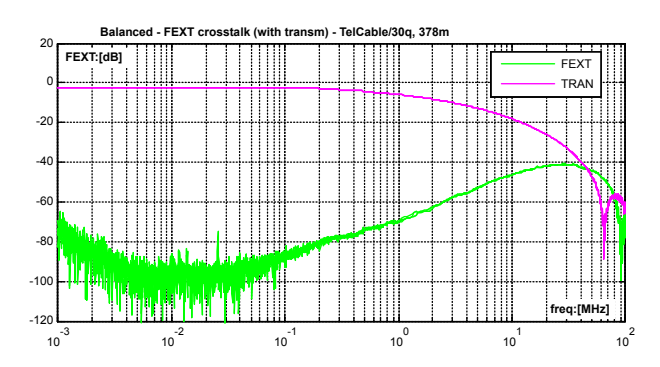


Fig. 1. Transmission and FEXT, measured in both directions of a 378m multi quad telephony cable.

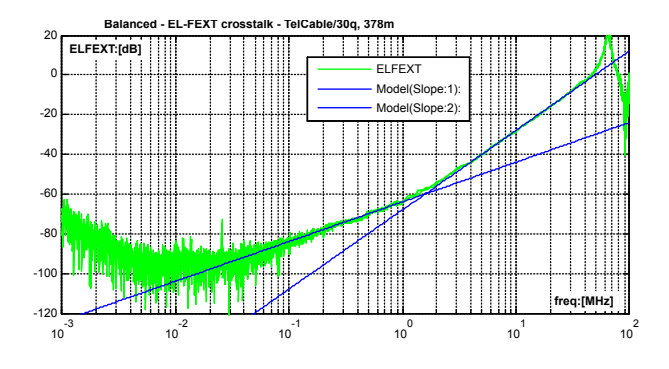


Fig. 2. The dual slope behavior of the magnitude of the EL-FEXT (20 and 40 dB/decade).

Figure 3 shows two curves, each of them representing the measured phase of the EL-FEXT from a first wire pair to the second one in the same quad, and from the second to the first pair. This phase has a random appearance up to about 100kHz, where the first order slope dominates. This is indicative for a random origin of the first order behavior of the EL-FEXT. Above about 2 MHz, the phase converges to constant values up to about 60MHz; the band where

the second order slope dominates. The lack of randomness is indicative for a more deterministic origin of the second order behavior of the EL-FEXT. Moreover, the pairs of forward crosstalk coupling functions in the quad converge to opposite sign, a behavior that is typical within quads of cables where the dual-slope effect is clearly visible.

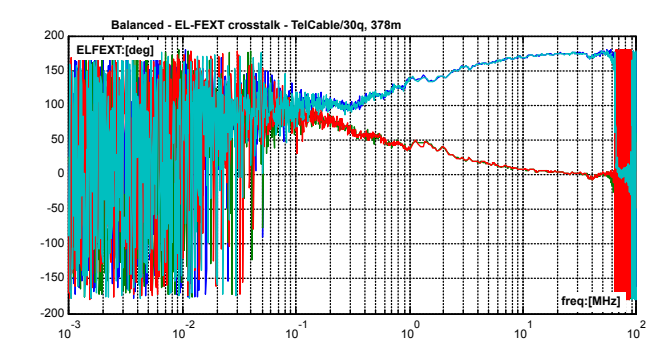


Fig. 3. The phases of both forward EL-FEXT transfers in a quad converge to opposite signs between 1 and 60 MHz.

The existence of the first order slope (20 dB/decade) is well known [6], [7] and is caused by imperfections in the symmetry of each quad, which are randomly distributed along the cable length. The model proposed in chapter 3 shows in chapter 5 that the second order slope (40 dB/decade) is caused by the repetitive variation of capacitance from each wire to the cable shield (and other conductive surroundings) due to the twist in each quad. This twist is a deterministic effect and regular along the full cable length.

3 SIMULATION APPROACH

The wire pairs in a multi quad cable are organized in groups of four wires, as shown in figure 4, and surrounded by a common shield. Each pair (1-2) or (3-4) of opposite wires is being used in a balanced mode. If the geometry of such a quad is a perfect square, and the quad is far away from the shield and other quads, then the symmetry will cause that the crosstalk from one balanced pair (1-2) to the other balance pair (3-4) in the same quad is zero. But this is not the case in practice, for instance when the quad is in the vicinity of a shield. Then each wire has an additional capacitance to that shield (and to other quads) as well, as shown in the circuit equivalent of figure 4.

This capacitance is not equal for each wire and thus deteriorates the overall symmetry of the quad. This is one of the reasons why quads are twisted so that each wire approaches the shield as often as the other three over each twist length. This makes all wire capacities to shield equal on average, restores the balance on average and reduces the overall crosstalk significantly.

To model this twisting effect, we consider the cable as a long cascade of very short cable sections of four wire structures. If the length of each section is short enough (compared to the twist length) then they can be assumed as piece-wise uniform over its length. Each section may have different uniformity but this will be repetitive if the wires are regularly twisted. By treating each uniform section with four wires as an 8-port (using the shield as common),

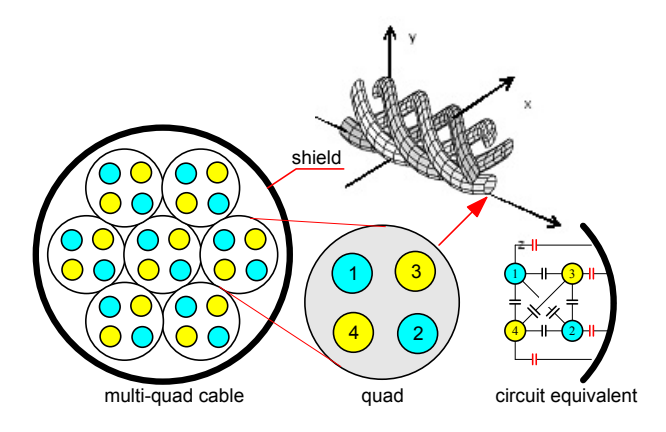


Fig. 4. A multi-quad cable is organized in groups of four wires positioned in a square, and each quad is twisted many times over its full length. Opposite wires (1-2) and (3-4), are used for (balanced) transmission, and each wire has a capacitance to all the other wires and to the common shield.

cascade them all over the full cable length as 8-ports, and extract from that cascade the overall balanced transfers of the wire pairs, then we obtain the transfer functions of interest.

3.1 MODELING UNIFORM CABLE SECTIONS

A complete modeling of each uniform cable section can be obtained via the well-known multi-conductor transmission line equations [19]:ch3, [4], [20]. When z denotes the longitudinal position in this cable structure, then the vectors of voltages \mathbf{U} and currents \mathbf{I} are at each position z given by the matrix collection:

$$\frac{\partial}{\partial z} \mathbf{U}(z) = -\mathbf{Z}_s \cdot \mathbf{I}(z)$$

$$\frac{\partial}{\partial z} \mathbf{I}(z) = -\mathbf{Y}_p \cdot \mathbf{U}(z)$$
(1)

In these expressions is \mathbf{Z}_s the series impedance matrix per unit length and \mathbf{Y}_p the shunt admittance matrix. If we split them into their real and imaginary parts we may phrase them as $\mathbf{Z}_s = \mathbf{R}_s + j\omega\mathbf{L}_s$ and $\mathbf{Y}_p = \mathbf{G}_p + j\omega\mathbf{C}_p$. Note that all these matrices are in principle non-zero and frequency dependent. This description can be thought of an alternating cascade of infinite thin (inductive) series networks and (capacitive) shunt networks, as depicted in figure 5.

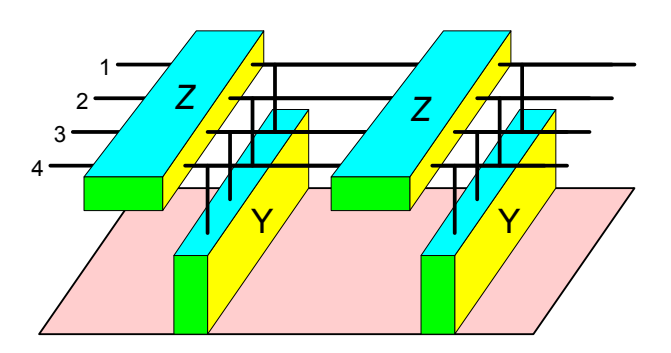


Fig. 5. An alternating cascade of infinite thin networks can represent a uniform cable.

The series impedance matrix \mathbf{Z}_s is dominantly inductive in nature representing the series inductance (per unit length)

of individual wires and some magnetic coupling between them. By adding series resistors we can account for the cable loss. The shunt admittance matrix \mathbf{Y}_p is dominantly capacitive in nature representing all capacitive coupling (per unit length) between the wires and the shield. Dielectric losses are assumed to be zero, meaning that \mathbf{G}_p is assumed to be zero. A circuit diagram representing this for a uniform 4-wire structure surrounded by a shield, is shown in figure 6, and this concept can easily be generalized for more wires.

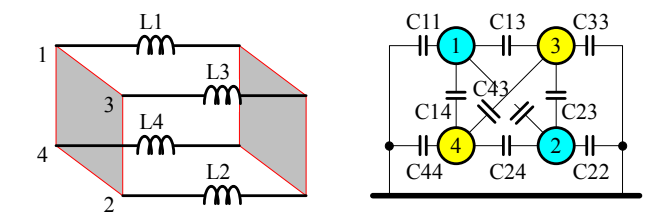


Fig. 6. The Z-matrix is inductive in nature and the Y-matrix is capacitive in nature.

To model \mathbf{Y}_p from this example structure we assume $\mathbf{G}_p=0$ and assume \mathbf{C}_p to be frequency-independent. In other words, we assume only ideal lumped capacitors between the wires and/or shield, where $C_{rk}=C_{kr}$ denotes the lumped capacitance per unit length between wire r and k, and C_{kk} between wire k and the common shield. By transforming this lumped circuit description into its Y-parameter representation, we obtain the desired (symmetric) \mathbf{Y}_p for a 4-wire structure:

$$\mathbf{Y}_{p} = j\omega \cdot \mathbf{C}_{p} = j\omega \cdot \begin{bmatrix} \sum C_{1} & -C_{12} & -C_{13} & -C_{14} \\ -C_{21} & \sum C_{2} & -C_{23} & -C_{24} \\ -C_{31} & -C_{32} & \sum C_{3} & -C_{34} \\ -C_{41} & -C_{42} & -C_{43} & \sum C_{4} \end{bmatrix}$$
(2)

Where
$$\Sigma C_r = C_{r1} + C_{r2} + C_{r3} + C_{r4} = C_{1r} + C_{2r} + C_{3r} + C_{4r}$$
.

To model the imaginary part of \mathbf{Z}_s from our example structure we assume L_s to be frequency-independent, and its real part by a simple frequency-dependency for \mathbf{R}_s , In other words we assume for L_s only ideal lumped inductors that are all magnetically coupled, and for \mathbf{R}_s resistors in series with these inductors. Similarly to C_p we can model L_s independently by assuming lumped inductance and coupling values. However this approach can easily result in cable models predicting properties that are physically impossible. Therefore it is often more convenient to evaluate \mathbf{L}_s indirectly via \mathbf{C}_p by making additional assumptions on the effective dielectric scaling values of the associated capacitors. These are the ratios between the lumped capacitance values of the actual structure and the lumped values of the same structure in the hypothetical situation that all dielectric is vanished. Just as if only the metallic parts are left and floating in vacuum. If that hypothetical structure has C_{p0} as capacitance matrix and \mathbf{L}_{s0} as associated inductance matrix then the free-space matrix relation $\mathbf{L}_{s0} \times \mathbf{C}_{p0} = \mathbb{I}/c_0^2$ holds [19]:eq3.37, [4]:eq4. In this expression is I the identity matrix and $c_0 = 3 \cdot 10^8$ m/s the speed of light in vacuum. And since our structure is assumed to have no magnetic materials inside, \mathbf{L}_s and \mathbf{L}_{s0} are the same. If $\epsilon_{rk} = \epsilon_{kr}$ represent the effective dielectric scaling values of the lumped capacitors $C_{rk}=C_{kr}$ then we can create $\mathbf{L}_s=\mathbf{L}_{s0}=1/c_0^2 imes inv(\mathbf{C}_{p0})$

$$\mathbf{L}_{s} = \frac{1}{c_{0}^{2}} \cdot \begin{bmatrix} \sum_{C} CE_{1} & -C_{12}/\epsilon_{12} & -C_{13}/\epsilon_{13} & -C_{14}/\epsilon_{14} \\ -C_{21}/\epsilon_{21} & \sum_{C} CE_{2} & -C_{23}/\epsilon_{23} & -C_{24}/\epsilon_{24} \\ -C_{31}/\epsilon_{31} & -C_{32}/\epsilon_{32} & \sum_{C} CE_{3} & -C_{34}/\epsilon_{34} \\ -C_{41}/\epsilon_{41} & -C_{42}/\epsilon_{42} & -C_{43}/\epsilon_{43} & \sum_{C} CE_{4} \end{bmatrix}^{-1}$$

$$\text{Where } \sum_{C} CE_{r} = C_{r1}/\epsilon_{r1} + C_{r2}/\epsilon_{r2} + C_{r3}/\epsilon_{r3} + C_{r4}/\epsilon_{r4}$$
(3)

To complete the modelling of \mathbf{Z}_s with its real part, we also assume \mathbf{R}_s as the result of 4 lumped resistors, in series with the four lumped inductors in \mathbf{L}_s . This simplifies \mathbf{R}_s into a diagonal matrix since the dielectric is assumed to act as perfect insulator. These resistors are to be frequency-dependent to account for the skin-effect in the wires, and a simple truncated series expansion in $\sqrt{\omega}$ can model this dependency quite well. If each wire r adds an equal series resistance to each inductor, then this diagonal matrix \mathbf{R}_s becomes:

$$\mathbf{R}_{s} = \left(R_{s0} + \sqrt{\frac{\omega}{\omega_{0}}} \cdot R_{s1} + \frac{\omega}{\omega_{0}} \cdot R_{s2} + \cdots \right) \cdot \begin{bmatrix} 1 & 0 & 0 & 0 \\ 0 & 1 & 0 & 0 \\ 0 & 0 & 1 & 0 \\ 0 & 0 & 0 & 1 \end{bmatrix}$$
(4)

Where R_{s0} to R_{s2} are all constants and $\omega_0=2\pi\cdot 1MHz$

The nominal values in table 1 are chosen to offer a good match between our model and the cable measurements in the figures 1, 2 and 3. They are found via a trial and error approach. The series expansion for the resistors is truncated after the third term.

TABLE 1 Nominal parameter values, to simulate a section

$C_{11} \approx C_{22} \approx C_{33} \approx C_{44}$	C_c	10	pF/m
$C_{31} \approx C_{42} \approx C_{32} \approx C_{41}$	C_p	22	pF/m
$C_{21} \approx C_{43}$	C_q	9.5	pF/m
$\varepsilon_{11} \approx \varepsilon_{22} \approx \varepsilon_{33} \approx \varepsilon_{44}$	ε_c	3.3	
$\varepsilon_{13} \approx \varepsilon_{42} \approx \varepsilon_{32} \approx \varepsilon_{41}$	ε_p	2.5	
$\varepsilon_{21} \approx \varepsilon_{43}$	ε_q	3.1	
R_{s0}	R_{s0}	0.0863	Ω/m
R_{s1}	R_{s1}	0.130	Ω/m
R_{s2}	R_{s2}	0.018	Ω/m

With only 9 nominal values per unit length, a full multiport parameter descriptions of this symmetric and uniform line can be evaluated from the matrices \mathbf{Z}_s and \mathbf{Y}_p , for instance by using the methods described in [19]:ch7. In our case, we transformed them all into single wire s-parameters for the full cable and from that into mixed mode parameters for the balanced wire pairs.

3.2 MODELLING THE TWIST IN THE QUAD

The full cable however is not uniform because the twist in the wires causes the distance between each wire and the shield to vary with the z position in that cable. As a result the capacity from wire to shield varies regularly from a minimum to a maximum value, and back. We have approximated this over a full twist length by cascading n uniform but slightly different sections, where n varied between 4 and 64. The four capacitance values from the wires to the shield vary gradually as well with the section position while all other values in table 1 are kept at their nominal value. These capacitances are roughly inversely

proportional with the distance d, and the twist causes each distance to vary in a harmonic manner over a full twist length ΔL . Therefore this variance in segment k has been modelled as:

$$C_{11} = C_c / (1 + \Delta_c \cdot \sin(2\pi \cdot k/n \cdot \Delta L))$$

$$C_{22} = C_c / (1 - \Delta_c \cdot \sin(2\pi \cdot k/n \cdot \Delta L))$$

$$C_{33} = C_c / (1 + \Delta_c \cdot \cos(2\pi \cdot k/n \cdot \Delta L))$$

$$C_{44} = C_c / (1 - \Delta_c \cdot \cos(2\pi \cdot k/n \cdot \Delta L))$$
(5)

Where Δ_c is a chosen "shield unbalance" factor, ΔL the twist length, n the number of steps per twist, k an integer index of the section, and C_c a nominal value taken from table 1. The full cable can subsequently be approximated by repeating this cascade as often as needed for creating the full cable length (over 16000 sections in our example cable). This is a brute force approach, but allows us to analyze various cable properties.

TABLE 2
Parameter values used to simulate the twisting

Sections per twist	"n"	n	16	
Twist length	"dL"	ΔL	37	cm
Shield unbalance	"dc"	Δ_c	0.55	

4 SIMULATION ACCURACY

4.1 MATCH BETWEEN MODEL AND DATA

The modeling approach of the previous chapter in combination with the nominal values from table 1 and 2 offers a close prediction of the measured cable properties of our example cable. Figure 7 illustrates how close the magnitudes of measured and modelled transmission and far end crosstalk can be with above mentioned values. It shows two measured and two modelled curves, one representing the transmission and the other representing the far end cross talk in/to a wire pair of a quad. Both show a good match up to high frequencies and even the dip in the transmission around 65MHz is well predicted. The match between the curves in figure 7 become weaker for the highest frequencies, and is most pronounced by the deviation of the measured and modelled dip around 90MHz. This is probably caused by the fact that we have ignored that the velocity factor of this cable (ratio between propagation speed and the speed of light) is a bit frequency dependent. Since all geometric imperfections of the quad were ignored, except for the twisting, these dips are apparently caused by the interaction between twist and shield.

Figure 8 shows the match between measured and modelled phase of the EL-FEXT in both directions. Our model predicts a phase of 0 and 180 degrees between the two EL-FEXT curves in forward direction and this holds for the frequencies above about 2 MHz (from where the second order effect dominates the crosstalk) until about 60 MHz (from where the EL-FEXT has approached its asymptotic value of 0dB.

4.2 IMPACT OF STEPS PER TWIST

To verify if the number n of homogeneous sections per twist is large enough, we simulated the same cable length

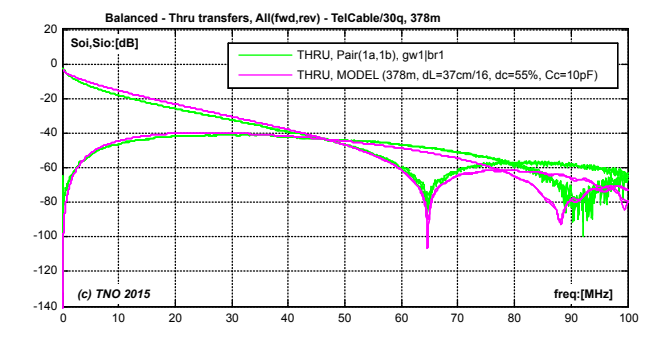


Fig. 7. Match of transmission and FEXT magnitudes, between model and measurement.

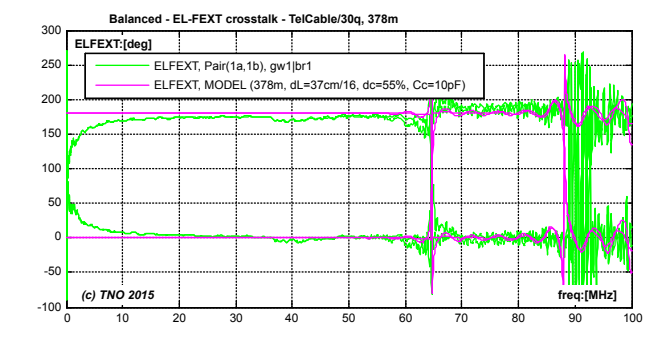


Fig. 8. Match of EL-FEXT phase, between model and measurement.

several times with an increasing number n. Figure 9 shows the simulated transfer and FEXT crosstalk of a 378m loop when we simulate it with n=4, 16 and 64 sections per twist respectively. This figure illustrates that this number hardly influences the result and that even a simulation with just 4 section per twist is adequate.

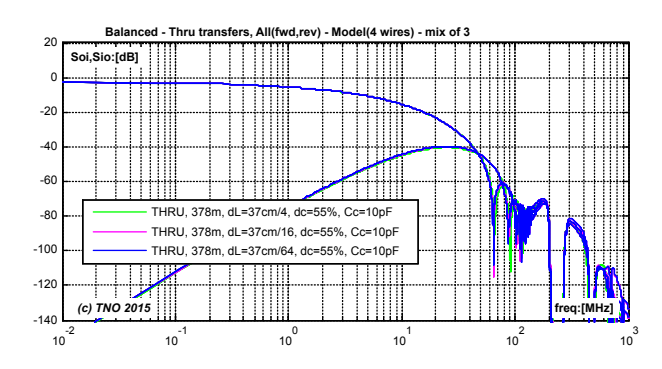


Fig. 9. A simulation with only 4 steps per twist offers similar result as a simulation with 64 steps per twist.

5 SENSITIVITY ANALYSIS

Now the model has proven to be reliable, we can use it to analyze the impact of changing some design parameters of the cable. This includes the impact of designing a cable with a tighter/looser twist or smaller/bigger variations of wire capacity to shield, or the impact of that nominal capacitance

5.1 SENSITIVITY TO TWIST LENGTH ΔL

Figure 10 shows the simulated results on the same loop when the twist length ΔL varies from 3 to 300cm. It shows

three curves, each of them representing EL-FEXT (ratio between FEXT and direct transmission) at another twist length (distance of a full 360° turn of a quad). All other parameters are assumed to be at the nominal values of table 1 and 2, so the quad is assumed to be perfectly symmetrical causing the first order slope (20 dB/decade) to be absent.

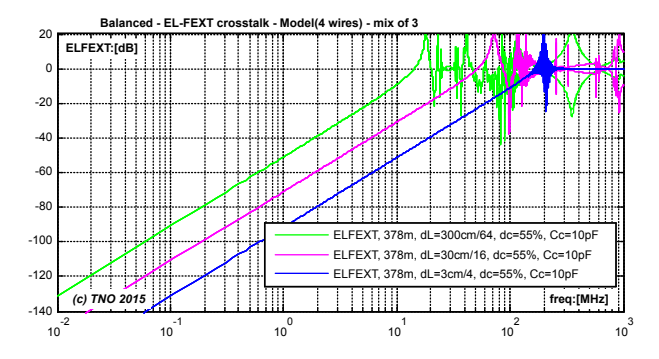


Fig. 10. An increase of twist-length by a factor 10 increases the EL-FEXT by 20 dB.

A first observation is that the slope of the second order EL-FEXT is accurately 40dB/dec over a very wide frequency interval. Another observation is that when the twist becomes tighter, the magnitude of this second order effect drops. A decrease of twist length by a factor 10 results in 20dB reduction of EL-FEXT. In other words: the EL-FEXT is proportional to the twist length. In addition, when the second-order EL-FEXT approaches the value one, the "meandering" around that asymptotic value becomes seemingly random in appearance.

5.2 SENSITIVITY TO SHIELD UNBALANCE Δ_C

Figure 11 shows the EL-FEXTs on the same loop when the variation between minimum and maximum capacitance between from wire to shield changes. It shows five curves where the shield unbalance Δ_c (as defined in table 2) varies in steps from 1% to 80%. This shield unbalance appeared to have a significant impact on the second order EL-FEXT. Each increase by a factor 10 causes 40dB increase in EL-FEXT. But in all cases the slope of the second order EL-FEXT remains accurately 40dB/decade over a very wide frequency interval.

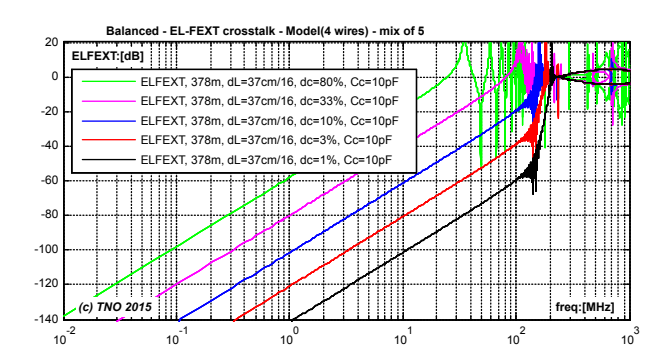


Fig. 11. An increase of the unbalance in capacity to shield by a factor 10 increase the EL-FEXT by 40 dB.

5.3 SENSITIVITY TO CAPACITANCE TO SHIELD

The nominal capacitance between wire and shield is not only determined by the nominal distance but also by the wire gauge and the dielectric in-between. Figure 12 shows four curves of EL-FEXT, where the (nominal) capacity C_c varies from 0.1pF to 100 pF. And all other parameters remain as defined in table 1 and 2. This time, the EL-FEXT does not change linearly with this capacity. In our example, it changes about 20dB from 0.1 to 1pF, 18dB from 1 to 10pF and about 9dB from 10 to 100pF.

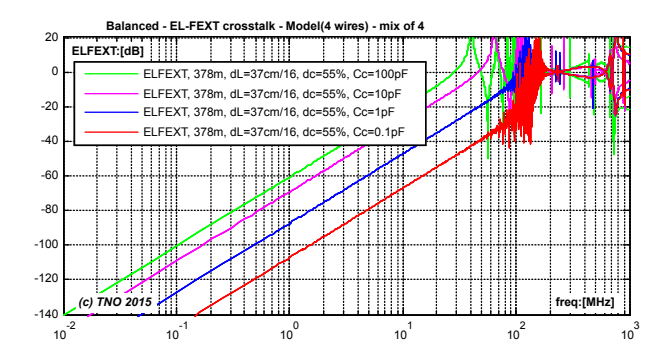


Fig. 12. An increase of the nominal capacitance between wire and shield increase the EL-FEXT in a non-linear way.

6 SIMPLIFIED SYSTEM MODEL FOR FEXT

For system performance calculations on DSL systems a simplified approximate model of EL-FEXT as function of the frequency cable and length is often adequate. The legacy model [17,20] is not adequate anymore for higher frequencies. It only accounts for the first order effect, and scales that first order EL-FEXT proportionally with the root of the cable length. To extend such a model with a second order effect as well we will first study how the second order effect scales with the loop length before we propose a simple extension.

6.1 INFLUENCE OF CABLE LENGTH ON EL-FEXT

The overall EL-FEXT increases with the cable length and is a combination of both the first and the second order behavior of the EL-FEXT. So far we have assumed in our modelling that the quad is in perfect symmetry to suppress the first order effect completely. This has emphasized the contribution of the second order behavior. The second order effect is more deterministic in nature. This makes it plausible that the (second order) EL-FEXT increases proportionally with the cable length. In practice, however, there are always small deviations from this perfect symmetry, and this contributes to the first-order behavior. Such deviations are dominantly random in nature, but a deterministic fragment cannot be excluded since a quad may have a regular deformation by its winding around a common core in a multi-quad telephony cable. If however this randomness dominates in the first order effect, then the EL-FEXT is assumed to increase proportionally with the square-root of the cable length (in a statistical sense). This is the classic assumption on EL-FEXT modelling [6], [7].

6.2 SIMULATING LENGTH DEPENDENCY

To prove the statements of the previous section, we will make our model more realistic to cover both the first and the second order effect. We have added random variation of capacitances around there nominal values, and apply these random changes to each small (uniform) section of the cascade calculation. This required a brute force cascade calculation of a huge number of uniform sections, where the capacitors C_p and C_q are randomly "jittered" for about 1% around their deterministic values table 1. This causes an additional first order behavior of the EL-FEXT

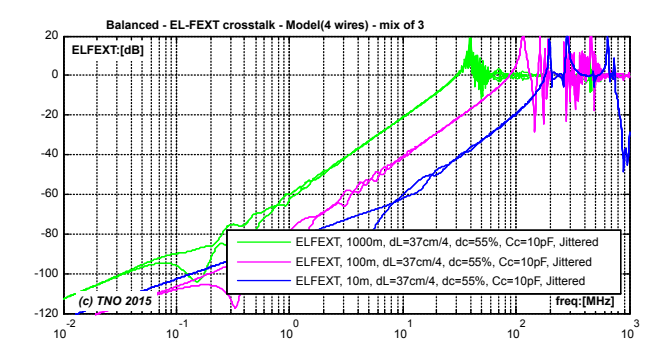


Fig. 13. Simulated EL-FEXT magnitude as function of the loop length.

Figure 13 shows three EL-FEXT curves from these brute force simulations, where the loop length varies in steps from 10 via 100 to 1000m. The low frequency part of these curves (below about 1 MHz) show that the first order EL-FEXT increases a bit random with the loop length. Roughly 10dB when the length increase by a factor 10. This demonstrates that the first order EL-FEXT increase roughly proportionally with the square root of the cable length, and this increase holds only in a statistical sense. The mid band frequencies of these curves (between about 1 and 100MHz) show that the second order EL-FEXT increases consistently by 20dB when the length increases by a factor 10. This demonstrates the expected linear increase of the EL-FEXT with the loop length. At higher frequencies, all EL-FEXT curves meander almost randomly around the value of 0dB.

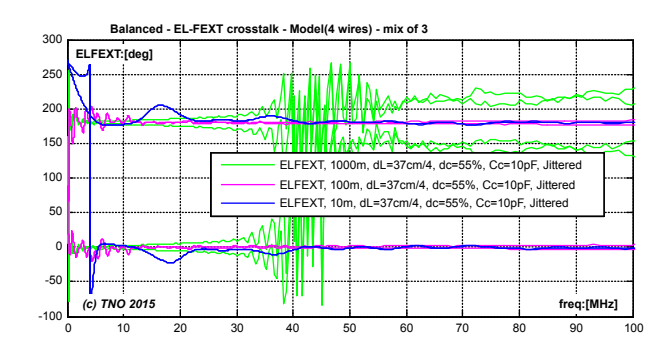


Fig. 14. Simulated EL-FEXT phase as function of the loop length; they have opposite values in the same direction.

Figure 14 shows two groups of curves, representing the phase of the two forward EL-FEXT curves in the same quad. In all cases they have roughly opposite values around 0 and 180 degrees over the frequency band where the second order effect dominates.

6.3 ENHANCED APPROXIMATING EL-FEXT MODEL

For system performance calculations on DSL systems, the brute force approach is a bit overkill, while the use of a simple transfer function $H_{ELFEXT}(j\omega,L)$, to approximate the EL-FEXT as function of frequency and cable length L, is often more adequate. The legacy model [6], [7] for that is a first order transfer function and is too simple for higher frequencies. Therefore we propose to extend it by using the transfer function of a second order high-pass filter. The following second order transfer function models the magnitude of the EL-FEXT much better, since it supports both the first and second order slope, has an asymptotic limitation for higher frequencies at 0dB, scales the first order slope with the root of the cable length and scales the second order slope linearly with the cable length. The transfer function has an insignificant overshoot near 0 dB.

$$\begin{split} H_{ELFEXT}\left(j\omega,L\right) = \\ = & \left\| \frac{k_1(L) \cdot \left(\frac{j\omega}{\omega_0}\right) + k_2(L) \cdot \left(\frac{j\omega}{\omega_0}\right) 2}{1 + \left(k_1(L) + \sqrt{k_2(L)}\right) \cdot \left(\frac{j\omega}{\omega_0}\right) + k_2(L) \cdot \left(\frac{j\omega}{\omega_0}\right) 2} \right\| \end{split}$$
 where $k1(L) = K_{XF1} \cdot \sqrt{L/L_0}$, and $k_2(L) = K_{XF2} \cdot \sqrt{L/L_0}$

In this expression are ω_0 and L_0 arbitrary scaling constants (e.g. 1 MHz and 1 km) and are K_{XF1} and K_{XF2} empirical values for matching the EL-FEXT characteristics between particular wire pairs of interest. To model our example cable, values like $K_{XF1}=-68.2 \mathrm{dB}$ and $K_{XF2}=-76.6 \mathrm{dB}$ both normalized to 1 MHz and 1 km cable, are adequate. When $K_{XF2}=0$ this enhanced model approximates the legacy model for EL-FEXT, since K_{XF1} is usually <<1.

7 Conclusions

It is well-known that the crosstalk in telephony cabling increases with the frequency, but the awareness that the increase of the EL-FEXT becomes much stronger above a certain frequency (40dB instead of 20dB per decade) was raised only recently [9], [8] and contributed to the ITU standardization group ITU-T SG14/Q4. This increase puts strong demands on vectoring engines of DSL modems to let VDSL and G.fast make efficient use of higher frequencies. We elaborated on a full-8-port model, to quantify various characteristics of this dual slope behavior of EL-FEXT in these cables. Our model did not only demonstrate that the second order effect is caused by the interaction between twist and shield, but also showed that (a) an increase of twist length by a factor 10 will increase the EL-FEXT by 20dB, (b) an increase of shield unbalance by a factor 10 will increase the EL-FEXT by 40dB, (c) an increase of the average capacitance to shield will also increase the EL-FEXT significantly but that effect is not linear, and (d) that the second order effect is a pure deterministic effect and thus increases proportionally with the cable length. The understanding of this phenomenon brought us to propose an adequate enhancement to the commonly used simplified model of EL-FEXT [6], [7] for supporting system calculations on the performance of DSL systems.

REFERENCES

- [1] P. Odling, T. Magesacher, S. Host, P. Borjesson, M. Berg, and E. Areizaga, "The fourth generation broadband concept," *IEEE Communications Magazine*, vol. 47, no. 1, pp. 62–69, 2009.
- [2] R. v. d. Brink, Boschma, and Popova, "Wideband transfer and crosstalk measurements on twisted pair cables," TNO Contribution 11BM-021 to ITU-T SG15/Q4, Apr 2011.
- [3] R. v. d. Brink, "Wideband modelling of twisted pair cables as two-ports," TNO Contribution 11GS3-028 to ITU-T SG15/Q4, Sept 2011.
- [4] Magesacher, "Mtl a multi-wire transmission line modelling tool-box," *Journal of Computer and Electrical Engineering*, vol. 5, no. 1, pp. 52–55, Feb 2013.
- [5] D. Acatauassu, S. Host, C. Lu, M. Berg, A. Klautau, and P. Borjesson, "Simple and causal copper cable model suitable for g.fast frequencies," *IEEE Transactions on Communications*, vol. 62, no. 11, pp. 4040–4051, 2014.
- [6] Spectral management on metallic access networks; Part 2: Technical methods for performance evaluations, ETSI Std. TR 101 830-2, Rev. V1.2.1, 2008.
- [7] Transmission systems for communications. Bell Telephone Labs, 1971, 4th edition.
- [8] R. v. d. Brink, "Far-end crosstalk in twisted pair cabling; measurements and modeling," TNO Contribution 11RV-022 to ITU-T SG15/Q4, Nov 2011.
- [9] —, "Dual slope behaviour of el-fext," TNO Contribution 2012-02-4A-038 to ITU-T SG15/Q4, Feb 2012.
- [10] Eriksson, Berg, and Lu, "Equal length fext measurements on pe05 cable," Ericsson Contribution 11RV-054R1 to ITU-T SG15/Q4, Richmond, Nov 2011.
- [11] "Equal-length fext measurements on pe05 cable," Huawei Contribution COM 15 - C 1864 to ITU-T SG15/Q4, Nov 2011.
- [12] Bruyssel and Maes, "Dual slope behaviour of el-fext," ALU Contribution 2012-06-4A-033 to ITU-T SG15/Q4, May 2012.
- [13] Humphrey, "On dual slope fext observations," BT Contribution 2012-05-4A-021 to ITU-T SG15/Q4, May 2012.
- [14] Humphrey and Morsman, "Fext cable measurements," BT Contribution 2012-05-4A-025 to ITU-T SG15/Q4, May 2012.
- [15] Muggenthaler and Tudziers, "El-fext analysis," DT Contribution 2012-06-4A-041 to ITU-T SG15/Q4, May 2012.
- [16] Bongard, "Dual slope elfext behaviour on swiss cables," Swisscom contribution 2013-01-Q4-042 to ITU-T SG15/Q4, Feb 2013.
- [17] Schneider, Kerpez, Starr, and Sorbara, "Transfer functions, input impedance and noise models for the loop end," Cosigned contribution bbf2014.066 to Broadband Forum, March 2014.
- [18] R. v. d. Brink, "Enabling 4gbb via hybrid-ftth, the missing link in ftth scenarios," TNO Contribution bbf2010.1395 to Broadband Forum, Dec 2010.
- [19] C. Paul, Analysis of Multiconductor Transmission Lines. Wiley-IEEE Press, 2008.
- [20] Kozarev, Strobel, Leimer, and Muggenthaler, "Modeling of twisted-pair quad cables for mimo applications," Lantiq/DT Contribution bbf2014.467 to Broadband Forum, June 2014, (updated from bbf2014.377 and bbf2014.117).



Rob F.M. van den Brink graduated in Electronics from Delft University in 1984, and received his PhD in 1994. He works as a senior scientist within TNO on broadband access networks. Since 1996, he has played a very prominent role in DSL standardisation in Europe (ETSI, FSAN), has written more than 100 technical contributions to ETSI, and took the lead within ETSI-TM6 in identifying / defining cable models, test loops, noise models, performance tests, and spectral management. He is the editor of an ETSI-TM6

reference document on European cables, and led the creation of the MUSE Test Suite, a comprehensive document for analyzing access networks as a whole. He also designed solutions for Spectral Management policies in the Netherlands, and created various DSL tools for performance simulation (SPOCS, www.spocs.nl/en) and testing that are currently in the market. He has been Rapporteur/Editor for ETSI since 1999 (on Spectral Management: TR 101 830), Board Member of the MUSE consortium (2004-2008, www.ist-muse.org) and is now (since 2009) Work Package leader various projects of the Celtic 4GBB Consortium (2009-2017, www.4gbb.eu). This consortium initiated the development and standardization of G.fast. All about you and the what your interests are.